Effect of PEO Grafts on the Surface Properties of PEO-Grafted PU/PS IPNs: AFM Study

J. H. Kim and S. C. Kim*

Center for Advanced Functional Polymers, Korea Advanced Institute of Science and Technology, 373-1 Gusong-dong, Yuseong-gu, Daejon 305-701, Korea

Received July 26, 2002

ABSTRACT: The change of the interfacial phenomena of muticomponent polymeric systems based on self-reorganization is very important for many applications of them. Specially, when they are used for biomedical application, the change of surface properties in water is a key factor because they are mostly used in the aqueous environment of the human body. An interpenetrating polymer network (IPN) is a mixture of network polymers. The morphology of an IPN can be controlled to obtain materials with nanoscale domains, and the morphology once formed is permanent due to the presence of the physical interlocking between the networks. In this study, surface compositional mapping was attempted with atomic force microscopy (AFM) images of poly(ethylene oxide)-grafted polyurethane/polystyrene IPNs (PEO-grafted PU/PS IPNs) to investigate the structural change under water, and the effect of hydrophilic PEO pendant chains on the change of local elasticity and surface energy of the IPN under water was studied by using the "force−distance (*F*/*D*) analysis" of AFM. The compositional mapping in water showed that the area fraction of the hydrophilic PU-rich phase was increased by PEO grafting, but the structural reorganization did not occur. From the result of *F*/*D* analysis in water, the mobile and flexible pendant PEO chains increased the surface elasticity and softness of PU/PS IPNs. The crystallinity also affected the surface hardness of the dried PEO-grafted PU, but it did not when the samples were swollen in water.

Introduction

Atomic force microscopy (AFM) was first applied to polymer surfaces in 1988, shortly after its invention.[1] AFM has become an advanced microscopic method for examining polymer materials for such applications as engineering plastics, paint and coating, rubber, packaging, fiber, and a wide range of consumer goods. Initially, AFM studies were aimed at visualization of polymer morphology, nanostructure, and molecular order, with investigations having been performed on a large number of polymer samples.[2,3] More recently, the spectrum of AFM applications to polymers has been broadened substantially from relatively simple visualizations of morphology to more advanced examinations of polymer structures and properties on a nanometer scale due to the discovery of new AFM capabilities. AFM has some advantages over other microscopic techniques. For example, scanning and transmission electron microscopy (SEM, TEM) image only biologically inactive, dehydrated samples and generally require extensive sample preparation, such as staining or metal coating. AFM eliminates these requirements, and in many cases AFM can directly obtain the three-dimensional information. AFM can also measure nanoscale interactive forces, e.g., ligand−receptor binding, ionic force, etc.

In addition, AFM also allows observation of changes of the surface properties of polymers under water, for example, structural changes, and change of surface energy under water. These changes in the surface properties under water are very important factors related to the biomedical applications of polymers because they are mostly used in the aqueous environment of the human body. In 1999, Nakahama et al. reported the nanoscale phase restructuring at the outermost surface of amphiphilic poly[2-hydroxyethyl methacrylate-*block*-4-(7-octenyl)styrene] diblock copolymers under dry and wet conditions.[4,5] This phenomenon had important implications because the associated polymeric material was an excellent candidate for the artificial polymeric prosthesis.

Many amphiphilic microphase-separated polymeric materials have been proposed for use in biomedical applications. Their amphiphilic character is very useful in the suppression of the adhesion of blood coagulation factors, for example proteins, platelets, lymphocytes, etc., by prohibiting the glycoproteins from excessively accumulating on a local position of the surface. From this point of view, in 1994, our research group also proposed that hydrophilic PU/hydrophobic PS IPNs be used in biomedical applications, and it was reported that the amphiphilic material exhibited good blood compatibility as well as excellent mechanical properties.[6−8] Also, the effect of the degree of phase separation on blood compatibility, with controlled morphology, was investigated. The IPN surfaces developed microphase-separated structure with the same likelihood as the amphiphilic diblock copolymers did previously, but the hydrophilic phase and hydrophobic phase interlocked, and thus structural stability and insensitivity to environmental change would be expected. Recently, we introduced mobile hydrophilic pendant PEO chains on the IPNs to enhance the blood compatibility under conventional physiological conditions, and we reported that the grafting of mobile pendant PEO chains on the IPN suppressed platelet adhesion and protein adhesion on the IPN due to the "molecular cilia effect" of the pendant chains.[9−11] In this study, surface compositional mapping was attempted with AFM images of PEO-grafted PU/PS IPNs by using recently developed AFM techniques. We also investigated the effect of hydrophilic

* To whom correspondence should be addressed: e-mail kimsc@mail.kaist.ac.kr.

10.1021/ma0212137 CCC: $25.00
Published on Web 03/22/2003

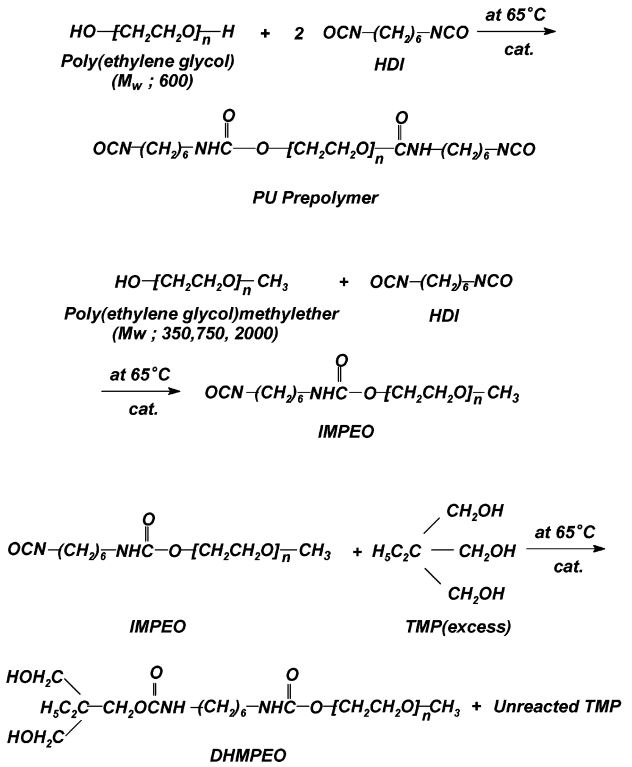

Figure 1. Syntheses of PU prepolymer, IMPEO, and DHMPEO.

PEO pendant chains on the local elasticity and surface energy of the IPN by using the "force−distance analysis" of AFM.

Experimental Section

Materials. Poly(ethylene glycol) (PEG, M_w = 600, Junsei Chemical Co., Ltd., ≥99.97%), poly(ethylene glycol) methyl ether (PEGME, M_w = 350, 750, 2000, Aldrich Chemical Co., Inc.), 1,4-butanediol (1,4-BD, Junsei Chemical Co., Ltd., ≥99.7%), and trimethylolpropane (TMP, Acros Organics, 98%) as a cross-linking agent for the PU network were degassed at 65 °C for 12 h under vacuum to remove moisture before use. Styrene monomer (SM, Showa Chemical Co., Ltd.) was purified to remove quinone, the inhibitor by the conventional method.[12] Hexamethylene diisocyanate (HDI, Tokyo Kasei Kogyo Co., Ltd., 98%), divinylbenzene (DVB, Aldrich Chemical Co., Inc., 80%) as a cross-linking agent for the PS network, and benzoyl peroxide (BPO, Fluka Chemika, ≥97%) as an initiator for the polymerization of styrene were used without further purification.

PU Prepolymer. Diisocyanate-terminated PU prepolymer was prepared by reacting 1 equiv of HDI with 2 equiv of dropping PEG (M_w = 600) (Figure 1). For grafting of PEO to the polyurethane network, IMPEO (isocyanate-methoxy-terminated poly(ethylene oxide)) and DHMPEO (dihydroxy-methoxy-terminated poly(ethylene oxide)) were synthesized sequentially as follows. IMPEO was prepared by reacting 1 equiv of poly(ethylene glycol) methyl ether (PEGME) with 1 equiv of HDI. Three kinds of PEGMEs, of which the molecular weights were 350, 750, and 2000, respectively, were used to introduce the various lengths of PEO pendant chains to the PU network. After that, DHMPEO was prepared by reacting 1 equiv of IMPEO with excess trimethylolpropane (TMP). The unreacted TMP would function as the cross-linking agent during the formation of PU network. The molecular structures of IMPEO and DHMPEO were investigated by NMR spectroscopy.

PU Homopolymer. Ungrafted PU homopolymer was prepared by reacting the diisocyanate-terminated PU prepolymer with 1,4-butanediol (1,4-BD) as a chain extender and trimethylolpropane (TMP) as a cross-linking agent. 0.05 wt % of dibutyltin diaurate (T-12) was added as a catalyst. 1,4-BD and TMP were mixed and degassed before reaction. PU prepolymer, 1,4-BD, and TMP were mixed vigorously by a high-torque stirrer in a 250 mL beaker. The air bubbles entrapped during the mixing were then removed under vacuum for about 3 min. The mixture was cast in a glass plate mold, with a silicon spacer of 1 mm thickness. The cast mixture was polymerized at 60 °C for 5 h and then postcured at 100 °C for 2 h in a convection oven. PU homopolymers with PEO pendant chains were prepared in the same way as the preparation of the ungrafted PU, but DHMPEO was used instead of 1,4-BD.

PU/PS IPNs. The mixture of PU prepolymer, 1,4-BD, TMP, SM, DVB, and BPO was degassed under vacuum for a few seconds and then cast in a glass mold with a silicon spacer. The PU network was formed first in a convection oven at 60 °C for 5 h, and then the PS network was formed in a convection oven at 80 °C for 10 h. The PU/PS IPN formed were postcured in a convection oven at 100 °C for 2 h additionally. PU/PS IPNs with pendant PEO chains were prepared using DHMPEO instead of 1,4-BD as a chain extender. Three kinds of DHMPEO of various molecular weights were used to change the length of PEO grafts. The prepared samples are described in Table 1.

Surface Morphology. The morphology of the top surface of the PU/PS IPNs was investigated by using scanning probe microscopy (SPM, DI NanoScope IIIa). SPM measurement was performed in air with an etched silicon probe having a length of 125 μm; the spring constant was from 20 to 100 N/m. Scanning was carried out in Tapping mode at a frequency of about 0.5 Hz. The surface morphology of PEO-grafted PU/PS IPNs under water was also observed by using an SPM equipped with an oxide-sharpened tip and liquid tip holder. The oxide-sharpened tip prevents micro air bubbles from adhering to the tip surface. PEO-grafted PU/PS IPNs were equilibrated with water before the experiment and then attached on the sample holder. Water was injected into the space between the sample and tip holder with a 1 mL syringe, and the scanning of the tip commenced at resonance frequency with water. The schematic diagram of the AFM study under water is shown in Figure 2.

Compositional Mapping. Compositional mapping was performed to investigate the area fraction of the PU-rich phase in the PEO-grafted PU/ PS IPN surfaces and the effect of the hydrophilic pendant PEO chains. This was done with AFM images of PEO-grafted PU/ PS IPNs in air and under water by using an off-line AFM image analyzer.

Elasticity and Adhesion Force of PEO-Grafted PU. The effect of the pendant PEO chains on the surface properties of PU/PS IPNs, for example, surface elasticity (hardness) and adhesion force, was easily investigated by using "force−distance analysis" (F/D analysis) of the SPM technique.[13−15] Figure 3 shows the principle of the experiment. In this experiment, the distance between sample and tip (Z-position) was gradually decreased and then increased without changing the horizontal position (XY-position). When there exists tip−

Table 1. Sample Notation

sample	mol wt of PEO used in the synthesis of PU prepolymer	mol wt of PEGME used in the synthesis of DHMPEO	weight fraction (wt/wt %)		
			pendant chains	PU network	PS network
IPN600-0	600			50	50
IPN600-350	600	350	14	43	43
IPN600-750	600	750	20	40	40
IPN600-2K	600	2000	36	32	32

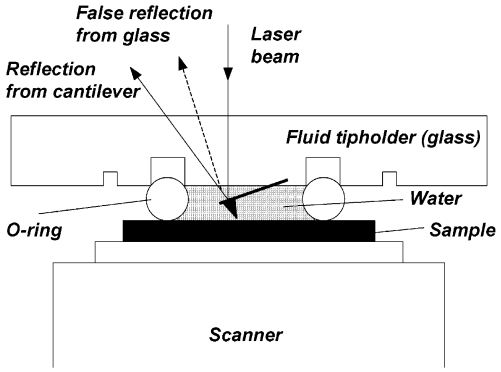

Figure 2. Schematic diagram of SPM measurement in water.

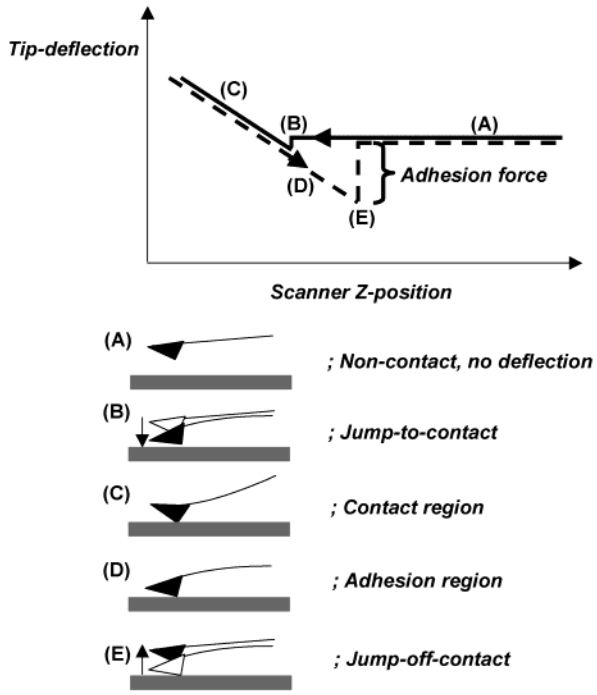

Figure 3. SPM (or AFM) "force−distance analysis".

sample interaction, the cantilever with the tip deflects until the elastic force of the cantilever equals the tip−sample force, and the system is in equilibrium. At point A, there is no interaction, and tip deflection does not occur. At point B, the tip jumps to contact the sample surface because most sample surfaces are covered by a thin layer of water. Mate et al. observed this, and they were able to measure the thickness of the adsorbed molecular layer of water.[16−19] The "jump to contact" disappears when the *F*/*D* analysis is carried out in water. Once the tip is in contact with the surface, cantilever deflection will increase (C). If the F/D analysis is carried out in water, the probe tip may indent the soft surface of a polymer, and the slope or shape of the contact part of the force−distance curve can provide information about the elasticity of the sample surface. After loading the tip to a desired force value, the process is reversed. As the cantilever is withdrawn, adhesion formed during contact with the surface causes the tip to adhere to the sample (D) some distance past the initial contact point on the approach curve (B). A key measurement of the AFM force curve is point E, at which the adhesion is broken and the cantilever comes free from the surfaces. This can be used to measure the rupture to break the adhesion, that is, the tip−sample adhesion force. If the tip is very hydrophilic, for example, an Si_3N_4 tip, the adhesion force indicates the surface hydrophilicity.

Interfacial Energy with Water. Interfacial energy between the surfaces of PU/PS IPNs, PU homopolymer, and the water was measured by an underwater captive bubble technique to correlate the results from AFM *F*−*D* analysis with surface hydrophilicity. The samples were equilibrated with distilled water for more than 24 h, and the static bubble contact angles of the surface−water−air and the surface−water−octane were then measured by a contact angle goniometer (Erma model G-I type) equipped with an oil droplet apparatus in water. Interfacial energy between the surface and the water was calculated from the geometric mean equation.

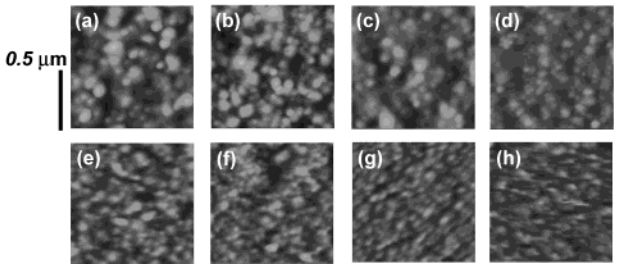

Figure 4. SPM images of surfaces of PEO-grafted PU/PS IPNs: (a)−(d) in air; (e)−(h) in water: (a), (e) IPN600-0; (b), (f) IPN600-350; (c), (g) IPN 600-750; (d), (h) IPN600-2K.

Results

Compositional Mapping. The morphology of the top surfaces of PU/PS IPNs in air and in water is shown in Figure 4. The surfaces of PU/PS IPNs showed microphase-separated sea-and-island morphology in all cases. The PS-rich phase domains were observed in the PU-rich phase matrix. The average diameter of the PS-rich domains decreased from 72 to 57 nm in air and from 66 to 41 nm in water, as the length of pendant PEO chains was increased. We identified that the hydrophilic phase was not washed off in water, and the microphase-separated structure remained stable in water. The macroscale rearrangement between both components at the water−surface interface was prohibited by the interlocking between the PU-rich and the PS-rich phases of PU/PS IPNs. The average diameter of the PS-rich was decreased in water, compared to that in air, because the tip−sample interaction was diminished in water, and tip deflection was decreased.

The swelling of the hydrophilic PU-rich phase in water changed the hydrophilic−hydrophobic balance in the surface morphology. The area fraction of hydrophilic PU-rich phase increased in water, as compared with that in air (Figure 5). IPN600-2K showed highest swelling in water, compared to other samples, and the area fraction of hydrophilic PU-rich phase reached about 65%.

Glass Transition and Crystallization. As we could know from the SPM images of the PEO-grafted PU/PS IPNs above shown, the effect of the pendant PEO chains on the properties of PU/PS IPNs was expected to be shown only on the PU-rich phase matrix because the hydrodynamic radius of the pendant PEO chains was much smaller than the distance between the PS-rich domains and the radius of them (Table 2). The Flory radius[20,21] of pendant chains and the distance between pendant chains were theoretically calculated and summarized in Table 2. Flory radius means the hydrodynamic radius of the hemisphere that a polymer chain, of which one end attaches to other surface or interface, occupies in a good solvent. In this study, the swollen cross-linked part of PU/PS IPNs was assumed as the immobile surface in water, and the mobile pendant PEO chains was assumed as the polymer chains of which one end was attached to the surface. The limit of low σ, the fraction of surface sites grafted, is particularly simple.

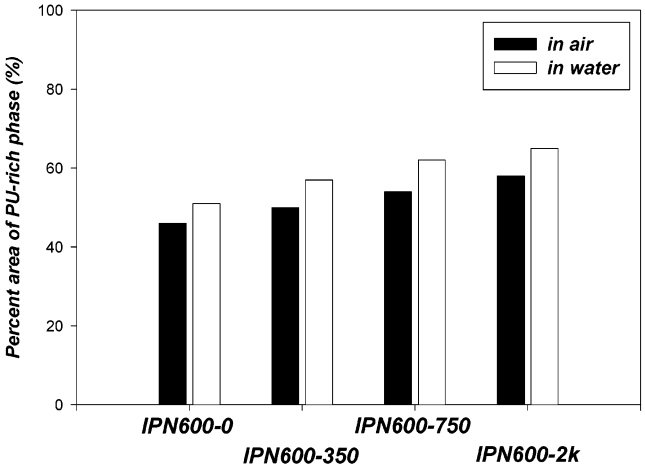

Figure 5. Area fraction of hydrophilic PU-rich phase in PU/PS IPNs. The area fraction was measured by using an image analyzer of SPM. The three-dimensional SPM image of sample surface was horizontally cut at the average height of the surface.

Table 2. Flory Radius of Pendant Chains and the Distance between Pendant Chains

sample	Flory radius,[a] R_F (nm)	D[b] (nm)
IPN600-350	1.401	16.35
IPN600-750	1.867	16.35
IPN600-2K	2.987	16.35

[a] Flory radius, $R_F = N^{3/5}a$ (N = the number of monomers, a = monomer size). [b] D = distance between pendant chains.

Each chain occupies roughly a half sphere with a radius comparable to the Flory radius (R_F) for a coil in a good solvent.

$R_F =$

$N^{3/5}a$ (N = the number of monomeric units; a = size of monomeric unit)

In this study, the size of the monomeric unit of pendant PEO, a, was determined referring to the result of Andrade,[22,23] which was calculated with X-ray and IR data, and the its value was about 0.278 nm. So, we focused on the properties of the PEO-grafted PU homopolymer which could represent the PU-rich phase in PU/PS IPNs easily.

The glass transition temperature slightly decreased by increasing the length of the pendant PEO chains in the dried PEO-grafted PU homopolymers (Figure 6a). Only PU-600-2K, which had the longest pendant PEO chains, showed high peaks of crystallization. As shown in Figure 6b, the crystallization peak of the dried PU-600-2K disappeared when it was swollen in water. Only the melting peaks of the ice absorbed in PEO-grafted and ungrafted PU homopolymers were observed, and the peak became deeper as the length of the pendant PEO chains increased. This indicated that the amount of absorbed water in the PU homopolymers increased by increasing the PEO chain length.

***F*/*D* Analysis in Air.** Figure 7a shows the *F*/*D* curve during approaching and receding of the SPM tip to the sample surface in air. The *Y*-axis represents cantilever deflection caused by tip−sample interaction. If the sample attracts the tip, the cantilever deflection becomes a negative value, and if the sample repulses the tip, it becomes positive. The elastic force of the tip can be calculated from the cantilever deflection with a known spring constant of the cantilever. At "jump to contact", the tip is attracted by the capillary force of the adsorbed moisture on the sample. The distance between the onset of this capillary attraction (the minimum point) and the point when the SPM tip reached the surface increased as the length of the pendant PEO chains was increased (Figure 7b). This indicates that the thickness of the adsorbed water layer increased with increasing of the length of pendant PEO chains. From that result, we could deduce that the long and hydrophilic pendant PEO chains readily attracted water molecules, as compared to short pendant PEO chains, which indicated that long pendant PEO chains could easily induce the microflow of water. At the contact region, the slope of the *F*/*D* curve represents the local hardness of the surface. In Figure 7b, the slope decreased as the surface became softer by increasing the length of the pendant PEO chains. In the case of PU-600-2K, the slope was steeper than that of PU-600-750, because of the high crystallinity of the PU-600-2K.

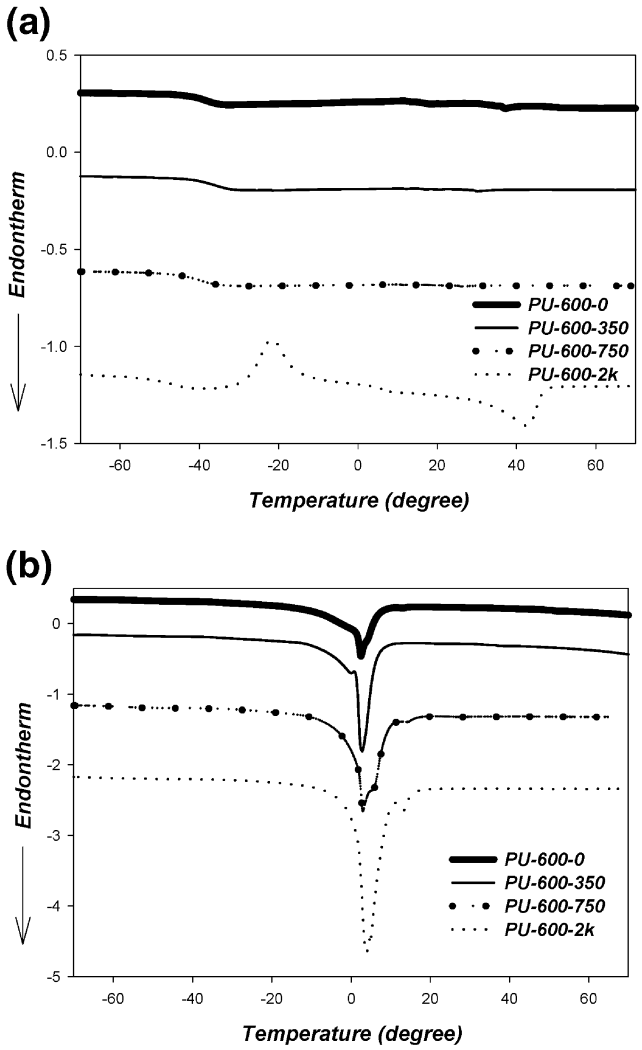

Figure 6. DSC thermogram of PEO-grafted PU homopolymer. Effect of pendant PEO length: (a) dried samples; (b) water-swollen samples.

As the cantilever is withdrawn, the adhesion between the surface and the tip caused the cantilever to deflect until the deflection force matches the adhesion force. This cantilever deflection before the detachment from the sample can be the quantitative measure of the adhesion between the tip and sample surface.[24,25] In

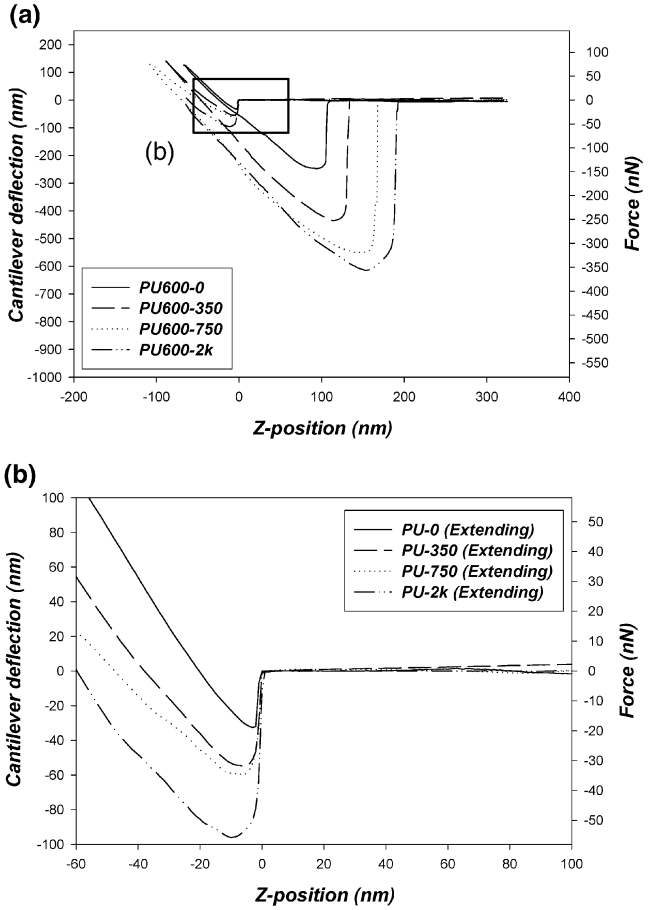

Figure 7. Force−distance curve of PEO-grafted PU in air. Effect of the length of pendant PEO chains: (a) *F*/*D* curve during approaching and receding of SPM tip to sample surfaces; (b) the magnified feature of *F*/*D* curve at "jump to contact".

Figure 7a, this tip−sample adhesion force was dramatically increased as the length of pendant PEO chain was increased because the surface hydrophilicity was increased and the thickness of the adsorbed water layer increased.

***F*/*D* Analysis in Water.** Figure 8 shows the *F*/*D* curve during approaching and receding of the SPM tip to the sample surfaces submerged in water. The "jump to contact" phenomenon disappears when the *F*/*D* analysis is carried out in water because the entire cantilever is completely submerged in water. Once the tip is in contact with the surface, cantilever deflection will increase. If the *F*/*D* analysis is carried out in water, the probe tip may indent the soft surface of polymer, and the slope or the force−distance curve can provide information about the elasticity of the sample surface. In this study, the slope of the force−distance curve in the contact region became lower as the length of pendant PEO chain was increased, indicating that the surface became softer (Figure 8b). When the PU-600-2K was swollen in water, the crystallinity disappeared and did not affect the surface hardness, compared to the case of the dried PU-600-2K.

During receding the tip from the sample in water, a small negative deflection (due to the adhesive force) was observed (Figure 8c). The adhesion increased as the length of pendant PEO chains was increased. This indicates that the hydrophilic pendant PEO chains on the surface attracted the silicone nitride tip and that

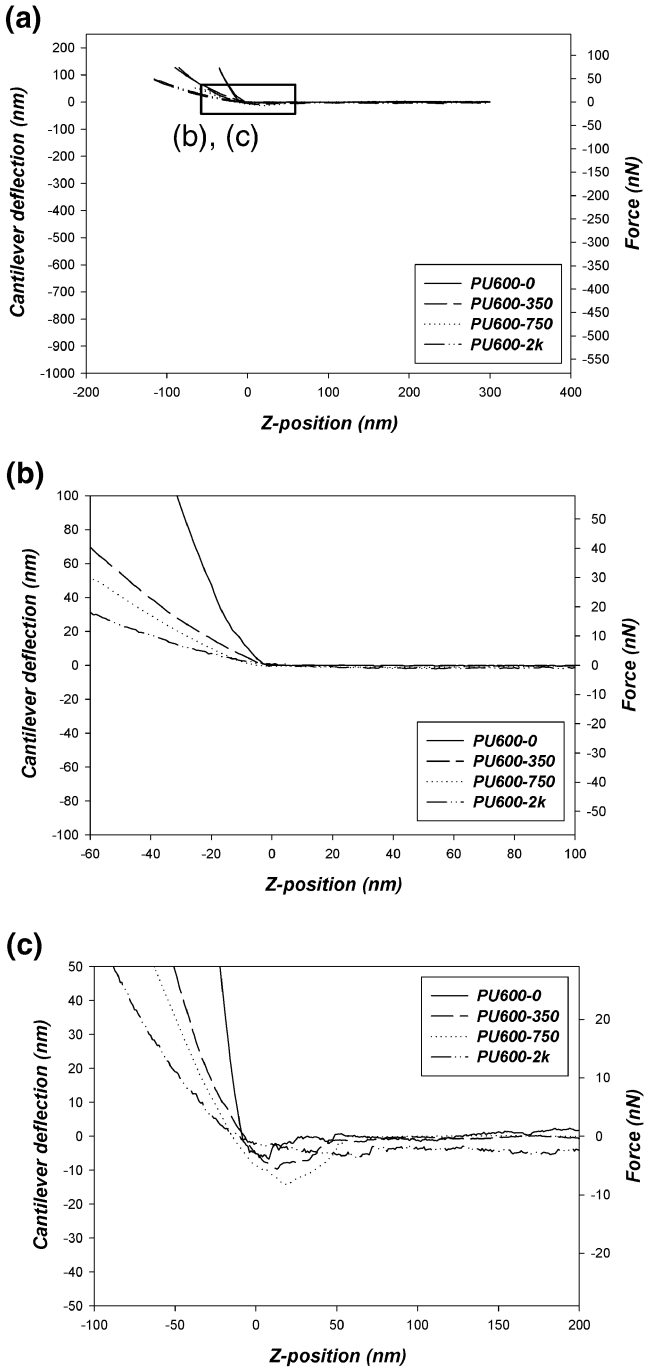

Figure 8. Force−distance curve of PEO-grafted PU in water: (a) *F*/*D* curve during approaching and receding of SPM tip to sample surfaces; (b) the magnified feature of the contact part of force−distance curve; (c) the magnified feature of the adhesion of SPM tip to the samples during withdrawing from the surface.

effect became more significant with increasing the length of the PEO chains.

Conclusions

PU homopolymers and PU/PS IPNs were synthesized with varying pendant PEO chain lengths. All the PU/PS IPNs had microphase-separated structures with PS-rich phase domains dispersed in the matrix of the PU-rich phase. The compositional mapping in water showed that the area fraction of the hydrophilic PU-rich phase was increased by PEO grafting. From the result of *F*/*D* analysis in air, it was found that the hydrophilic long

pendant PEO chains readily attracted the moisture in the air as compared with short pendant PEO chains, indicating that long pendant PEO chains could easily induce the microflow of water. The tip−sample adhesion force was dramatically increased as the length of pendant PEO chains was increased because the surface hydrophilicity was increased and the thickness of adsorbed water layer was increased. From the result of *F*/*D* analysis in water, we found that the mobile and flexible pendant PEO chains increased the surface elasticity and softness of PU/PS IPNs. The crystallinity also affected the surface hardness of the dried PEO-grafted PU, but it did not when the samples were swollen in water because the crystallization decreased so much (almost disappeared).

References and Notes

(1) Albrecht, T. R.; Dovek, M. M.; Lang, C. A.; Grutter, P.; Quate, C. F.; Kuan, S. N. J.; Frank, C. W.; Pease, R. F. W. *J. Appl. Phys.* **1998**, *64*, 1178.
(2) Magonov, S. N.; Whangbo, M. H. In *Surface Analysis with STM and AFM*; VCH Publishers: Weinheim, Germany, 1996.
(3) Zhong, Q.; Innis, D.; Kjoller, K.; Elings, V. B. *Surf. Sci. Lett.* **1993**, *290*, L668.
(4) Senshu, K.; Yamashita, S.; Mori, H.; Ito, M.; Hirao, A.; Nakahama, S. *Langmuir* **1999**, *15*, 1754.
(5) Senshu, K.; Yamashita, S.; Mori, H.; Ito, M.; Hirao, A.; Nakahama, S. *Langmuir* **1999**, *15*, 1763.
(6) Shin, Y. C.; Han, D. K.; Kim, Y. H.; Kim, S. C. *J. Biomater. Sci., Polym. Ed.* **1994**, *6*, 195.
(7) Shin, Y. C.; Han, D. K.; Kim, Y. H.; Kim, S. C. *J. Biomater. Sci., Polym. Ed.* **1994**, *6*, 281.
(8) Roh, H. W.; Song, M. J.; Han, D. K.; Lee, D. S.; Ahn, J. H.; Kim, S. C. *J. Biomater. Sci., Polym. Ed.* **1999**, *10*, 123.
(9) Kim, J. H.; Song, M. J.; Roh, H. W.; Shin, Y. C.; Kim, S. C. *J. Biomater. Sci., Polym. Ed.* **2000**, *11*, 197.
(10) Kim, J. H.; Kim, S. C. *J. Appl. Polym. Sci.* **2002**, *84*, 379.
(11) Kim, J. H.; Kim, S. C. *Biomaterials* **2002**, *23*, 2015.
(12) Perrin, D. D.; Armarego, W. L. F.; Perrin, D. R. In *Purification of Laboratory Chemicals*, 2nd ed.; Pergarnon Press: New York, 1980.
(13) Binnig, G.; Quate, C. F.; Gerber, C. H. *Phys. Rev. Lett.* **1986**, *56*, 930.
(14) Weisehorn, A. L. *Appl. Phys. Lett.* **1989**, *54*, 2651.
(15) Cappella, B.; Dietler, G. *Surf. Sci. Rep.* **1999**, *34*, 1.
(16) Mate, C. M.; Lorenz, M. R.; Novotny, V. J. *J. Chem. Phys.* **1989**, *90*, 7550.
(17) Sugawara, Y. In *Wear (Switzerland)*; Morioka: Japan, 1993.
(18) Thundat, T. *Surf. Sci.* **1993**, *294*, L939.
(19) Butt, M. J.; Jaschke, M.; Ducker, W. *Bioelectrochem. Bioenerg.* **1995**, *38*, 191.
(20) De Gennes, P. G. *Macromolecules* **1980**, *13*, 1069.
(21) De Gennes, P. G. In *Scaling Concepts in Polymer Physics*; Cornell University Press: Ithaca, NY, 1979.
(22) Jeon, S. I.; Lee, J. H.; Andrade, J. D.; De Gennes, P. G. *J. Colloid Interface Sci.* **1991**, *142*, 149.
(23) Jeon, S. I.; Andrade, J. D. *J. Colloid Interface Sci.* **1991**, *142*, 159.
(24) Hoh, J. H.; Revel, J. P.; Hansma, P. K. *Nanotechnology* **1991**.
(25) Hoh, J. H. *J. Am. Chem. Soc.* **1992**, *114*, 4917.

MA0212137